Evolution of mammalian Opn5 as a specialized UV-absorbing pigment by a single amino acid mutation*

Takahiro Yamashita[1,6], Katsuhiko Ono[2,6], Hideyo Ohuchi[3,6], Akane Yumoto[1], Hitoshi Gotoh[2], Sayuri Tomonari[4], Kazumi Sakai[1], Hirofumi Fujita[3], Yasushi Imamoto[1], Sumihare Noji[4], Katsuki Nakamura[5], and Yoshinori Shichida[1]

[1]Department of Biophysics, Graduate School of Science, Kyoto University, Kyoto 606-8502, Japan, [2]Department of Biology, Kyoto Prefectural University of Medicine, Kyoto 603-8334, Japan, [3]Department of Cytology and Histology, Okayama University Graduate School of Medicine, Dentistry and Pharmaceutical Sciences, Okayama 700-8558, Japan, [4]Department of Life Systems, Institute of Technology and Science, University of Tokushima Graduate School, Tokushima 770-8506, Japan, [5]Primate Research Institute, Kyoto University, Inuyama, Aichi 484-8506, Japan.

*Running title: *Molecular property and expression pattern of mammalian Opn5*

Correspondence should be addressed to Y.S. (shichida@rh.biophys.kyoto-u.ac.jp)

[6]These authors contributed equally to this work.

Keywords: Rhodopsin; Photoreceptors; Signal transduction; G proteins; Molecular evolution; non-visual photoreception

Background: Opn5 is considered to regulate non-visual photoreception in the retina and brain of animals.
Results: Mouse and primate UV-sensitive Opn5 along with retinoid isomerase are localized in the preoptic hypothalamus.
Conclusion: Mammalian Opn5 can function as a high-sensitivity photosensor in the deep brain with the assistance of 11-*cis*-retinal supplying system.
Significance: Mammals including humans may detect short-wavelength light within the brain via Opn5.

ABSTRACT

Opn5 is one of the recently identified opsin groups that is responsible for non-visual photoreception in animals. We previously showed that a chicken homolog of mammalian Opn5 (Opn5m) is a Gi-coupled UV sensor having molecular properties typical of bistable pigments. Here we demonstrated that mammalian Opn5m evolved to be a more specialized photosensor by losing one of the characteristics of bistable pigments, direct binding of all-*trans*-retinal. We first confirmed that Opn5m proteins in zebrafish, *Xenopus tropicalis*, mouse and human are also UV-sensitive pigments. Then we found that only mammalian Opn5m proteins lack the ability to directly bind all-*trans*-retinal. Mutational analysis showed that these characteristics were acquired by a single amino acid replacement at position 168. By comparing the expression patterns of Opn5m between mammals and chicken, we found that, like chicken Opn5m, mammalian Opn5m was localized in the ganglion cell layer and inner nuclear layer of the retina. However, the mouse and primate (common marmoset) opsins were distributed not in the posterior hypothalamus (including the region along the third ventricle) where chicken Opn5m is localized, but in the preoptic hypothalamus. Interestingly, RPE65, an essential enzyme for forming 11-*cis*-retinal in the visual cycle, is expressed near the preoptic hypothalamus of the mouse and common marmoset brain, but not near the region of the chicken brain where chicken Opn5m is expressed. Therefore, mammalian Opn5m may work exclusively as a short-wavelength sensor in the brain as well as in the retina with the assistance of an 11-*cis*-retinal-supplying system.

Opsins are the universal photosensitive proteins responsible for visual and non-visual photoreception in animals, and are G protein-coupled receptors (GPCRs) having a seven transmembrane α-helical structure. They contain vitamin A-derivative retinal as their

light-absorbing chromophore, and the retinal binds to a conserved lysine residue located at the center of helix VII through a Schiff base linkage. A variety of opsins have been identified so far and are classified into at least seven groups according to their sequence similarity (1-2). Opn5 is the most recently identified opsin in the human and mouse genomes (3) and is categorized in an independent group on the basis of its low sequence homology to the other opsin groups. Opn5 genes have been identified in various vertebrates from fishes to primates and are classified into several subgroups (4-5). Most mammals have only one Opn5 gene (Opn5m), whereas non-mammalian vertebrates have additional Opn5 genes. This is probably because of the nocturnal period in the early evolution of mammals, during which mammals lost several non-visual opsins as well as color opsin genes (6).

In our previous reports, we succeeded in the purification of recombinant Opn5 proteins obtained by the expression of chicken Opn5 genes and reported that these proteins are UV-sensitive bistable pigments that activate Gi-type of G protein (4,7). We also speculated from the complete conservation of the amino acid residues surrounding the chromophore between chicken and mammalian Opn5m proteins that mammalian Opn5m proteins should be UV-sensitive pigments, which was recently confirmed in mouse and human Opn5m proteins (8). In the present study, we compared the molecular properties of Opn5m proteins from zebrafish (fish), *Xenopus tropicalis* (amphibian), chicken (bird), mouse (mammal) and human (primate), paying particular attention to the differences between mammals and non-mammalian vertebrates. In addition, we also analyzed the expression patterns of mouse and primate (common marmoset) Opn5m and RPE65, an enzyme essential for generating 11-*cis*-retinal in the visual cycle (9-10), to compare with those of chicken Opn5m and RPE65.

EXPERIMENTAL PROCEDURES

Animals and ethics statement - Fertilized chicken eggs (*Gallus gallus domesticus*) were purchased from a commercial farm (Goto-furanjyo, Inc., Gifu, Japan; http://www.gotonohiyoko.co.jp/) and incubated at 37.5 °C in a humidified incubator until hatching. Post-hatch chicks were housed under a 12:12 light-dark cycle with food and water *ad libitum*. Postnatal and adult mice were purchased from Shimizu Laboratory Animal Center (ICR and C57BL/6 strains, Shizuoka, Japan). Animals were anesthetized and euthanized at Zeitgeber time 6-10. The eyes and brains of common marmosets were obtained through the Cooperation Research Program of Primate Research Institute, Kyoto University. The use of animals in these experiments was in accordance with the guidelines established by the Ministry of Education, Culture, Sports, Science, and Technology, Japan, and University of Tokushima and Kyoto Prefectural University of Medicine (chick; mouse, *Mus musculus domesticus*) or Kyoto University (common marmoset, *Callithrix jacchus*). The protocol was approved by the Committee on the Ethics of Animal Experiments of the University of Tokushima (Permit Number: 08089, 11091, 11120), Kyoto Prefectural University of Medicine (M22-197) or Kyoto University (2011-142, 2012-B-35). All surgery was performed under deep anesthesia (pentobarbital, 100 mg/kg body weight), and all efforts were made to minimize suffering.

Preparation of Opn5 proteins - The cDNAs of human (GenBank accession number; AY377391), mouse (AY318865), *Xenopus tropicalis* (XM_002935990), and zebrafish (*Danio rerio*) (AY493740) Opn5m were tagged by the epitope sequence of the anti-bovine rhodopsin monoclonal antibody Rho1D4 (ETSQVAPA) at the C-terminus and were inserted into the mammalian expression vector pCAGGS (11). Site-directed mutations were introduced by the QuikChange kit (Agilent Technologies) according to the manufacturer's method. The plasmid DNA was transfected into HEK293 cells using the calcium phosphate method. After 1 day of incubation, 11-*cis*- or all-*trans*-retinal was added to the medium (final retinal concentration, 5 μM) (7). After additional incubation for 1 day in the dark, the cells were collected. The pigments were extracted with 1% digitonin (for human and mouse Opn5m proteins) or 1% n-dodecyl-β-D-maltoside (DM) (for *Xenopus* and zebrafish Opn5m proteins) in buffer A (50 mM HEPES [pH 6.5] and 140 mM NaCl) and were purified using Rho1D4-conjugated agarose. The purified pigments were eluted with 1% digitonin (for human and mouse Opn5m proteins) or 0.02% DM (for Xenopus and zebrafish Opn5m proteins) in buffer A containing the synthetic

peptide that corresponds to the C-terminus of bovine rhodopsin. The expression levels of human and *Xenopus* Opn5m proteins were very low, and thus to obtain sufficient amounts of recombinant proteins we truncated 37 and 21 amino acid residues from the C-terminus of human and *Xenopus* Opn5m proteins, respectively.

Spectrophotometry and HPLC analysis - Absorption spectra were recorded at 10 °C (for human and mouse Opn5m proteins) or 0 °C (for *Xenopus* and zebrafish Opn5m proteins) with a Shimadzu UV-2400 spectrophotometer. The sample was irradiated with UV light through a UV-D35 glass filter (Asahi Technoglass), with yellow light through a Y-52 cutoff filter (Toshiba) or with orange light through an O-57 cutoff filter (Toshiba) from a 1 kW halogen lamp (Master HILUX-HR; Rikagaku). The absorption spectra of visible and UV light-absorbing forms of Opn5m proteins were calculated using the methods previously described (7). Briefly, the spectral region at wavelengths longer than the maximum of the main peak of the spectrum difference between the visible and UV light-absorbing forms of the pigment was best-fitted with a template spectrum previously described (12-13). The best-fitting spectrum was considered to be the visible light-absorbing form of the pigment. The absorption spectrum of the UV light-absorbing form was then calculated by adding the visible light-absorbing form to the difference spectrum. The chromophore configurations of the sample were analyzed by HPLC (LC-10AT VP; Shimadzu) equipped with a silica column (150 x 6 mm, A-012-3; YMC) according to the previous report (14).

G protein activation assay - A radionucleotide filter-binding assay, which measures GDP/GTPγS exchange by G protein, was performed as described previously (4,7). All procedures were carried out at 0 °C. The assay mixture consisted of 50 mM HEPES (pH 7.0), 140 mM NaCl, 5 mM $MgCl_2$, 1 mM DTT, 0.01% DM, 1 μM [^{35}S]GTPγS and 2 μM GDP. Mouse Opn5m pigments after reconstitution with 11-*cis*-retinal were purified in 0.02 % DM in buffer A for the assay. Purified mouse Opn5m pigments (final concentration: 300 nM) were mixed with G protein solution (final concentration: 600 nM) and were kept in the dark or irradiated with UV light for 1 min or with subsequent yellow light (>500 nm) for 1 min. After irradiation, the GDP/GTPγS exchange reaction was initiated by the addition of [^{35}S]GTPγS solution to the mixture of the pigment and G protein. After incubation for the indicated time in the dark, an aliquot (20 μl) was removed from the sample into 200 μl of stop solution (20 mM Tris/Cl (pH 7.4), 100 mM NaCl, 25 mM $MgCl_2$, 1 μM GTPγS and 2 μM GDP), and it was immediately filtered through a nitrocellulose membrane to trap [^{35}S]GTPγS bound to G proteins. The amount of bound [^{35}S]GTPγS was quantitated by assaying the membrane with a liquid scintillation counter (Tri-Carb 2910 TR; PerkinElmer).

Antibodies - Specific antibodies were raised to the N-terminus of mouse Opn5m and the C-terminus of human Opn5m using guinea pigs. Each polyclonal antibody was commercially produced against a 15-amino-acid synthetic peptide conjugated to Keyhole Limpet Hemocyanin by Protein Purify Ltd. (Gunma, Japan), according to their standard procedures (mouse Opn5m: MALNHTALPQDERLPC; human Opn5m: CVRKSSAVLEIHEEWE). We confirmed that the sequence of this portion of human Opn5m (the C-terminus) is identical to that of common marmoset Opn5m deposited in the public database. We also confirmed that this isoform of human Opn5m cDNA was isolated from human retina cDNA (Marathon-Ready cDNA, Clontech) with 3'RACE. These antibodies were affinity purified prior to use by Protein Purify Ltd. The primary antibodies used in this study included: guinea pig anti-chick Opn5m antibody (7), and rabbit anti-RPE65 antibody (a gift from Dr. Rosalie K. Crouch, Medical University of South Carolina, USA) (15). We performed western blotting analysis using the antibodies and confirmed that the anti-mouse and human/monkey Opn5m antibodies recognized the recombinant proteins of full-length mouse and human Opn5m expressed in HEK293 cells, respectively (Fig. 1). The secondary antibody used for immunostaining in this study was Alexa Fluor 488 anti-guinea pig IgG (A-11073, Life Technologies Corp.).

Fixation and sectioning - The animals were perfusion-fixed with 4 % paraformaldehyde in phosphate-buffered saline (PBS) under deep pentobarbital anesthesia, and the eye and brain

were quickly dissected, post-fixed for 2 to 3 h (for eyes) or 16 h (for brain) in the same fixative at 4 °C and then transferred to 20 % sucrose until they sank. After embedding the samples in optimal cutting temperature compound (Sakura, Japan), the tissues were sectioned with a cryostat (Leica) at 20 μm thickness. Sections were thaw-mounted onto MAS-coated slides (Matsunami, Japan), dried in air for a few hours, and stored at -30 °C until use. The anatomy of the chick, mouse and common marmoset brain was determined according to (16), (17) and (18), respectively, and the nomenclature adopted in this study was based on these atlases and previous studies.

Immunohistochemistry - Fluorescent immunolabeling was performed using standard techniques. Briefly, all slides were blocked for 30 min at room temperature in PBS Triton X-100 (0.25 %) (PBST) with 5 % serum from the same species as the corresponding secondary antibodies. Primary antibodies were diluted in PBST with 5 % serum and secondary antibodies in PBS. All wash steps were performed 3 times with PBST for 5 min each. Primary antibodies (anti-N-terminus of mouse Opn5m [diluted 1:2000], anti-C-terminus of human Opn5m [diluted 1:2000], and anti-RPE65 [diluted 1:140] were incubated for 5 h at room temperature or for 16 h at 4 °C. Secondary antibodies were incubated for 1.5 h at room temperature and diluted 1:750. The cell nuclei were stained with 4',6-diamidino-2-phenylindole (DAPI) (Vector Laboratories). The slides were mounted with anti-fade mountant, Vectashield (Vector, H-1500). Fluorescent images were collected using a Leica TCS-SP5 confocal laser-scanning microscope, excitation 405, 488, and 543 nm with emission wavelengths of 424-489, 505-539, and 551-618 nm for DAPI, green, and Cy3, respectively.

In situ hybridization of mouse brain and retinal sections - Frozen sections (20 μm thickness) of mouse (ICR, postnatal day 0, 4 and 10, and 8 weeks, female; C57BL/6, 8 weeks, male and female) and adult common marmoset brain and retina were used. In situ hybridization was performed according to standard procedures. Briefly, digoxigenin (DIG)-labelled RNA probes were synthesized from full-length cDNA of mouse Opn5m (purchased from IMAGE cDNA Collection), common marmoset Opn5m (GenBank accession number; XM_002746623, synthesized by Medical & Biological Laboratories, Japan), mouse Rpe65 (AF410461; cloned by PCR from mouse eye) and human Rpe65 (BC075035; purchased from IMAGE cDNA Collection) using T7 T3 or Sp6 RNA polymerase. Sections were pre-treated with methanol for 2 hours and with proteinase K (20 μg/mL) for 40 min at room temperature. After prehybridization, sections were incubated with DIG-labeled RNA anti-sense or sense probes (15~30 ng/mL in hybridization buffer) at 65 °C overnight. They were washed with x1 SSC buffer containing 50 % formamide three times at 65 °C, and maleic acid buffer containing 0.1 % Tween 20, and subsequently incubated with anti-DIG antibody conjugated to alkaline phosphatase (1:2000 in PBS containing 0.1 % Triton X-100; Roche) overnight at 4 °C. Color was developed with BCIP/NBP. Sections were coverslipped and observed under a microscope.

Western blotting - Extract from full-length human or mouse Opn5m-transfected HEK293 cells was subjected to SDS-PAGE, transferred onto a polyvinylidene difluoride membrane, and probed with anti-human or mouse Opn5m antibody (1:1000) (Fig. 1). Protein extracts from mouse tissues were prepared as follows (8). Eight-week old male mice were anesthetized and perfused with ice-cold PBS. The tissues were dissected and solubilized in 1% DM in buffer B (50 mM HEPES [pH 6.5], 140 mM NaCl, 1 mM dithiothreitol, 1 mM EDTA, 4 mg/mL aprotinin, 4 mg/mL leupeptin, 0.1 mM phenylmethylsulfonyl fluoride). After centrifugation, the supernatant was collected for SDS-PAGE. Mouse Opn5m or RPE65 in the extracts from mouse neural retina, RPE, hypothalamus, other brain area, lung and liver was detected by anti-mouse Opn5m (1:1500) or RPE65 antibody (1:1000) (Fig. 7O, P)

RESULTS AND DISCUSSION

*Vertebrate Opn5m proteins reconstituted with 11-*cis*- or all-*trans*-retinal*

We first expressed recombinant proteins of Opn5m from four vertebrates, zebrafish, *Xenopus tropicalis*, mouse and human, in cultured cells and examined whether or not these pigments have molecular properties similar to those of chicken Opn5m. As already reported, chicken Opn5m is a UV-sensitive bistable pigment that forms 11-*cis*- and all-*trans*-retinal bound states, the latter of which activates Gi-type of G protein (7). We also

found that, although the apoprotein of Opn5m protein is extremely unstable, we could successfully obtain adequate amounts of chicken Opn5m pigment by adding 11-*cis*- or all-*trans*-retinal to the culture medium during the protein expression. Fig. 2C shows the photoreactions of chicken Opn5m that had been purified after incubation with 11-*cis*-retinal. The absorption spectrum of purified pigment exhibited UV and visible absorbances, indicating that the chicken Opn5m protein binds 11-*cis*-retinal to produce a UV light-absorbing form and also binds all-*trans*-retinal, which is formed by thermal isomerization of 11-*cis*-retinal in culture medium, to produce a visible light-absorbing form (Fig. 2H) (7). UV light irradiation of the pigment caused the conversion of the UV light-absorbing form to the visible light-absorbing form, and subsequent yellow light irradiation resulted in the complete conversion of the visible light-absorbing form to the UV light-absorbing form. The light-induced interconversion between the UV light- and visible light-absorbing forms could be observed repeatedly (Fig. 2C).

We performed similar experiments using zebrafish, *Xenopus*, mouse and human Opn5m proteins (Fig. 2A, B, D, E). The absorption spectra and photoreactions of zebrafish and *Xenopus* Opn5m were quite similar to those of chicken Opn5m. That is, the addition of 11-*cis*-retinal to the culture medium caused the production of UV light- and visible light-absorbing forms that were interconvertible by light (Fig. 2D, E). In contrast, incubation of mouse and human Opn5m proteins with 11-*cis*-retinal in the culture medium caused the production of only the UV light-absorbing form. In fact, UV light irradiation of mouse and human pigments caused the production of the visible-light absorbing form, and subsequent yellow light irradiation resulted in the production of the UV-light absorbing form, whose absorption spectrum overlapped with that of the dark state (Fig. 2A, B). The analysis of the retinal configurations of human Opn5m also showed that human Opn5m was exclusively reconstituted with 11-*cis*-retinal and UV light irradiation induced the retinal isomerization from 11-*cis* to all-*trans* form (Fig. 2K). Therefore, mouse and human Opn5m showed photoreversibility similar to that of chicken Opn5m but had no ability to directly bind all-*trans*-retinal.

The absorption maxima of the UV light-absorbing forms of these Opn5m proteins are all located at 360 nm (Fig. 2, *Insets*). In contrast, while the absorption maxima of visible light-absorbing forms of zebrafish, *Xenopus* and chicken Opn5m proteins are located at 474 nm, those of mouse and human Opn5m proteins are located at 469 nm (Fig. 2, *Insets*). These differences would reflect the differences of the ability to bind all-*trans*-retinal among these Opn5m proteins.

To confirm that mammalian Opn5m has no ability to directly bind all-*trans*-retinal, we performed similar expression experiments in the presence of all-*trans*-retinal instead of 11-*cis*-retinal in the culture medium (Fig. 2F-J). In zebrafish and *Xenopus* Opn5m proteins, we observed the production of visible light-absorbing forms that exhibited photoreactions identical with that of chicken Opn5m (Fig. 2H-J). On the other hand, we observed no pigments of mouse or human Opn5m under the present conditions (Fig. 2F, G). These results clearly showed that mammalian Opn5m proteins have no ability to directly bind all-*trans*-retinal.

We also confirmed that the visible light-absorbing form of mammalian Opn5m is the active state that couples with Gi (Fig. 3). Purified mouse Opn5m reconstituted with 11-*cis*-retinal activated Gi in a UV-light dependent manner, and lost the activity after subsequent yellow light irradiation. These alterations of the activity are consistent with the spectral changes shown in Fig. 2B, indicating that the visible light-absorbing form is the state activating G protein.

*Determination of amino acid residue that controls the ability of direct binding of all-*trans*-retinal*

Next, we attempted to identify the amino acid residue(s) whose substitution(s) resulted in loss of the ability to directly bind all-*trans*-retinal in mammalian Opn5m proteins. Comparison of the amino acid residues within 4.5 Å from the retinal, which are inferred from the 3D structures of bovine and squid rhodopsins (19-20), indicates that all the residues are completely conserved in mammalian and chicken Opn5m proteins. Thus, we compared the residues within 8 Å from the retinal among vertebrate Opn5m proteins. There are four residues that are conserved in human and mouse Opn5m proteins but not in non-mammalian Opn5m proteins (Table 1). We introduced each

corresponding mutation (T94S, T168A, D177S or I204V in the bovine rhodopsin numbering system) into mouse Opn5m and analyzed the alteration of the ability of direct incorporation of all-*trans*-retinal. Orange light irradiation of mouse Opn5m mutants incubated with all-*trans*-retinal led to a significant spectral change in T168A mutant, but not in wild-type or other mutants (Fig. 4A). The purified mouse Opn5m T168A had the peak of its absorption spectrum in the visible region and was photoconverted into a pigment whose absorption maximum was in the UV region (Fig. 4B). This spectral change is the same as those observed in non-mammalian Opn5m proteins reconstituted with all-*trans*-retinal. It should be noted that T168A mutation of mouse Opn5m resulted in red-shift of absorption maximum, close to those of non-mammalian Opn5m proteins. These results indicated that T168A mutation alters the all-*trans*-retinal binding ability as well as the electrostatic environment of the all-*trans*-retinal chromophore. In addition, we prepared A168T mutant of *Xenopus* Opn5m reconstituted with all-*trans*-retinal. The purified mutant exhibited no detectable peak of the absorption spectrum in the visible region and no spectral change after yellow light irradiation (Fig. 4B). Thus, this mutant lost the ability to directly bind all-*trans*-retinal. These data clearly showed that a single amino acid residue can modulate the ability of direct incorporation of all-*trans*-retinal as well as the electrostatic environment of the all-*trans*-retinal chromophore.

It has been reported that bovine rhodopsin cannot be reconstituted with all-*trans*-retinal to form the active state (21), because in neutral pH the equilibrium of inactive and active conformations of apoprotein of bovine rhodopsin is mostly biased toward the inactive conformation (22). Bovine rhodopsin has an alanine residue at position 168, the same as non-mammalian vertebrate Opn5m (Table 1). Therefore, the lack of ability of all-*trans*-retinal binding in bovine rhodopsin cannot be explained by the same molecular mechanism. Thus, the loss of all-*trans*-retinal binding ability in vertebrate visual opsin and mammalian Opn5m is the result of convergent evolution.

Alanine residue at position 168, which is well conserved in non-mammalian Opn5m proteins, is replaced into threonine residue in most mammalian Opn5m proteins. Exceptions are platypus (*Ornithorhynchus anatinus*) and opossum (*Monodelphis domestica*) Opn5m proteins, which have alanine residue in this position (Table 1). We speculate that A168T mutation occurred after the divergence of eutherian and metatherian mammals.

Localization of mammalian Opn5m in the retina and the brain

Mammals have several non-visual opsins, including Opn5m. The mRNA transcript of mammalian *Opn4 (melanopsin)* is exclusively expressed in the retina (23), whereas the mRNA of mammalian *Opn3 (encephalopsin)* is detected in the brain, but not in the retina (24). On the other hand, the mRNA of mammalian *Opn5m* is present in both the retina and brain (3,8,25), suggesting the multiple physiological roles of Opn5m. Therefore it is of interest to investigate the detailed expression patterns of mammalian Opn5m.

For this, first we performed in situ hybridization (ISH) and immunostaining on mouse retinal sections. Although our standard ISH technique could not detect *Opn5m* mRNA in the adult mouse retina, we observed the expression of *Opn5m* in the immature retina at postnatal day 1 (P1) and 11 (P11) (Fig. 5). Furthermore, we found Opn5m immunoreactive cells in the ganglion cell layer (GCL) of the adult retina (Fig. 6A). These signals were not seen when immunostaining was performed using antigen-adsorbed antibodies (Fig. 6B). We also performed immunohistochemical studies using the common marmoset retina and detected signals in the GCL and the inner nuclear cell layer (INL) (Fig. 6C, C', D). The expression pattern of Opn5m in the retina was similar between mouse and common marmoset, and consistent with those of mouse and rat seen in the previous studies (8,25). We previously observed immunostaining signals of Opn5m in the GCL and the INL of chick retina (7). Thus, the localization of Opn5m in the retina is conserved between mammals and chicken.

We next investigated the localization of *Opn5m* mRNA in the mouse brain. The results showed that *Opn5m* was expressed exclusively in the preoptic area, specifically, the median preoptic nucleus and medial preoptic area of the anterior hypothalamus (Fig. 7A-D). However, there was no *Opn5m* mRNA in the posterior hypothalamus or hippocampus (Fig. 8), whose counterparts in birds are known to contain photoreceptive cells (26). Moreover, our western blotting analysis showed that Opn5m protein was detected in the hypothalamus as

well as in the neural retina and other brain areas with the expected molecular weight (Fig. 7O).

*Comparison of localization of Opn5m and an 11-*cis*-retinol-generating enzyme, RPE65, in the mammalian brain*

We were surprised to find that mouse Opn5m is expressed in the preoptic hypothalamus, a deep brain region, because, in addition to the fact that UV light would scarcely penetrate into such a deep brain region, our biochemical analysis showed that mouse Opn5m protein has lost the ability to directly bind all-*trans*-retinal. We previously speculated that chicken Opn5m in the paraventricular organ (PVO) of the hypothalamus can be regenerated by all-*trans*-retinal binding and work as a photoreceptive molecule by absorbing visible light even without an 11-*cis*-retinal supply, because visible light can more easily be transmitted into the deep brain than UV light (7). However, mouse Opn5m cannot be regenerated by all-*trans*-retinal, and therefore it appears essential to have an 11-*cis*-retinal-supplying system (as in the visual cycle mechanism) in the vicinity. One important enzyme constituting the visual cycle is retinal pigment epithelium (RPE)-specific 65 kDa protein, RPE65. RPE65 in the RPE is involved in the conversion of all-*trans*-retinyl ester to 11-*cis*-retinol during the visual cycle (9-10). We therefore examined the expression domain of *Rpe65* in the mouse brain. We first confirmed that a high level of *Rpe65* mRNA is observed in the RPE of the adult mouse retina (Fig. 5). Then, we performed ISH on mouse brain sections and showed that *Rpe65* is expressed in the domains (Fig. 7G, H) near the *Opn5m*-expressing cells (Fig. 7E, F). In addition, by the western blotting analysis we detected multiple bands of putative RPE65 proteins in the dissected hypothalamus and other brain areas including a band of the same molecular weight as the band observed in the RPE (Fig. 7P). These results clearly showed that an RPE65-dependent retinal isomerization system is present near the region where Opn5m is expressed. It has been shown that lecithin retinol acyltransferase (LRAT), an enzyme that produces the substrate of RPE65 from all-*trans*-retinol in the visual cycle, is also expressed in the mouse brain, although its detailed expression pattern remains unknown (27). Thus LRAT may also contribute to Opn5m-RPE65 system in the brain.

Opn5m mRNA has also been detected in the human brain by RT-PCR analysis (3). Thus, to analyze the detailed distributions of *Opn5m* and *Rpe65* in the primate brain, we performed ISH on the common marmoset brain. We detected the expression of *Opn5m* mRNA in the anterior part of the medial preoptic area (Fig. 7I-K), which is in the vicinity of *Rpe65*-expressing domains (Fig. 7L-N). These results showed that Opn5m and RPE65 are expressed in the primate anterior hypothalamus.

We also examined the expression pattern of RPE65 in the chick brain by immunostaining. We found that anti-RPE65 antibody (Fig. 9D, E) detected a subset of ependymal cells lining the third ventricle (Fig. 9B, C). However, in the PVO region, there were no RPE65-immunoreactive cells in the ependymal layer, which abuts the Opn5m-immunoreactive neurons (Fig. 9A). These results support the notion that, in the chick brain, *Opn5m*-expressing cells of the PVO, which are thought to be responsible for the photoperiodism in birds (28-29), do not require assistance by RPE65 in generating 11-*cis*-retinal, as chicken Opn5m is a bistable pigment that can generate the 11-*cis*-retinal binding form from the all-*trans*-retinal binding form (7).

Photoreception within mammalian retina and brain via Opn5m

In this study, we demonstrated that not only rodents but also primates have the UV-sensitive Opn5 in the retina. Like the expression of melanopsin in a subset of retinal ganglion cells in mammals, including primates (30-31), the present findings suggest that retinal photoreception in mammals and primates is not restricted to classical rod and cone photoreceptor cells or intrinsically photosensitive retinal ganglion cells. More importantly, we demonstrated here the expression of Opn5m in the preoptic hypothalamus in the mouse and common marmoset deep brain. Mammalian Opn5m proteins exclusively bind 11-*cis*-retinal due to their loss of the ability to directly bind all-*trans*-retinal. Direct binding of all-*trans*-retinal causes the formation of the active state and elevates the G protein activation ability without light irradiation, which lowers the signal-to-noise ratio in light-dependent signaling. Light can penetrate the skull in several mammalian species, including human (26). And mammalian cerebral cortical tissues were

reported to respond to low-intensity light to regulate neurotransmitter release (32). In birds, the measurement of the light transmittance into the deep brain revealed that the hypothalamus can receive light enough to trigger opsin-mediated signal transduction (33) because of the high quantum yield of opsins (34). Thus, although there is no direct evidence to show that mammals actually utilize Opn5m to sense short-wavelength light, by the acquisition of exclusive 11-*cis*-retinal binding ability, Opn5m could function as a high-sensitivity photosensor within the mammalian brain. It is known that the sexually dimorphic nucleus is located in a cluster of cells of the preoptic area in the hypothalamus of the brain, and that it is related to sexual behavior in animals and its volume is usually larger in males than in females (35). Although we found no obvious differences in the amount of *Opn5m*-expressing cells between males and females (Fig. 10), Opn5m in this region might have a role in some sexual behaviors. In addition, the preoptic area of the hypothalamus is an important region to control the body temperature (36). Thus, Opn5m might contribute to light-dependent thermoregulation (37). In birds, Opn5m in the deep brain can regulate photoperiodic response (28). However, in mammals, visual opsins and Opn4 in the retina exclusively contribute to the control of melatonin release from the pineal gland (38-39), and thus Opn5m in the deep brain is not involved in photoperiodism (40). Compared with chicken Opn5m, mammalian Opn5m has changed its molecular property (i.e., has lost direct binding to all-*trans*-retinal) and its expression pattern within the brain, although it is difficult to precisely compare the areas of the brain between mammals and birds. The change of the molecular property and the expression pattern of Opn5m may be related with the difference of the physiological role of Opn5m between mammals and birds. Therefore, it is intriguing to speculate that Opn5m might have obtained a new physiological role in the early evolution of mammals, which will be the subject of our future research.

ACKNOWLEDGMENTS

We are grateful to Dr. Elizabeth Nakajima and Dr. Take Matsuyama for critical reading of the manuscript. We thank Professor Rosalie K. Crouch for the generous gift of the antibody against RPE65. We also thank Institute for Amphibian Biology, Hiroshima University, for the generous gift of *Xenopus tropicalis* through the National Bio-Resource Project of MEXT, Japan. This work was supported by the Cooperation Research Program of Primate Research Institute, Kyoto University. This work was also supported in part by Grants-in-Aid for Scientific Research (to T.Y., K.O., H.O., S.N., K.N. and Y.S.) and the Global Center of Excellence Program "Formation of a Strategic Base for Biodiversity and Evolutionary Research: from Genome to Ecosystem" of the Ministry of Education, Culture, Sports, Science and Technology (MEXT), Japan.

REFERENCES

1. Koyanagi, M., and Terakita, A. (2008) Gq-coupled rhodopsin subfamily composed of invertebrate visual pigment and melanopsin. *Photochem Photobiol* **84**, 1024-1030
2. Shichida, Y., and Matsuyama, T. (2009) Evolution of opsins and phototransduction. *Philos Trans R Soc Lond B Biol Sci* **364**, 2881-2895
3. Tarttelin, E. E., Bellingham, J., Hankins, M. W., Foster, R. G., and Lucas, R. J. (2003) Neuropsin (Opn5): a novel opsin identified in mammalian neural tissue. *FEBS Lett* **554**, 410-416
4. Ohuchi, H., Yamashita, T., Tomonari, S., Fujita-Yanagibayashi, S., Sakai, K., Noji, S., and Shichida, Y. (2012) A non-mammalian type opsin 5 functions dually in the photoreceptive and non-photoreceptive organs of birds. *PLoS One* **7**, e31534
5. Tomonari, S., Migita, K., Takagi, A., Noji, S., and Ohuchi, H. (2008) Expression patterns of the opsin 5-related genes in the developing chicken retina. *Dev Dyn* **237**, 1910-1922
6. Kuraku, S., and Kuratani, S. (2011) Genome-wide detection of gene extinction in early mammalian evolution. *Genome Biol Evol* **3**, 1449-1462
7. Yamashita, T., Ohuchi, H., Tomonari, S., Ikeda, K., Sakai, K., and Shichida, Y. (2010) Opn5 is a UV-sensitive bistable pigment that couples with Gi subtype of G protein. *Proc Natl Acad Sci U S A* **107**, 22084-22089
8. Kojima, D., Mori, S., Torii, M., Wada, A., Morishita, R., and Fukada, Y. (2011) UV-sensitive photoreceptor protein OPN5 in humans and mice. *PLoS One* **6**, e26388
9. Cai, X., Conley, S. M., and Naash, M. I. (2009) RPE65: role in the visual cycle,

human retinal disease, and gene therapy. *Ophthalmic Genet* **30**, 57-62
10. Kiser, P. D., and Palczewski, K. (2010) Membrane-binding and enzymatic properties of RPE65. *Prog Retin Eye Res* **29**, 428-442
11. Niwa, H., Yamamura, K., and Miyazaki, J. (1991) Efficient selection for high-expression transfectants with a novel eukaryotic vector. *Gene* **108**, 193-199
12. Govardovskii, V. I., Fyhrquist, N., Reuter, T., Kuzmin, D. G., and Donner, K. (2000) In search of the visual pigment template. *Vis Neurosci* **17**, 509-528
13. Lamb, T. D. (1995) Photoreceptor spectral sensitivities: common shape in the long-wavelength region. *Vision Res* **35**, 3083-3091
14. Tsutsui, K., Imai, H., and Shichida, Y. (2007) Photoisomerization efficiency in UV-absorbing visual pigments: protein-directed isomerization of an unprotonated retinal Schiff base. *Biochemistry* **46**, 6437-6445
15. Tang, P. H., Wheless, L., and Crouch, R. K. (2011) Regeneration of photopigment is enhanced in mouse cone photoreceptors expressing RPE65 protein. *J Neurosci* **31**, 10403-10411
16. Puelles, L. (2007) *The chick brain in stereotaxic coordinates : an atlas featuring neuromeric subdivisions and mammalian homologies*, Academic Press
17. Franklin, K. B. J., and Paxinos, G. (2007) *The mouse brain in stereotaxic coordinates, 3rd Edition*, Academic Press
18. Yuasa, S., Nakamura, K., and Kohsaka, S. (2010) *Stereotaxic atlas of the marmoset brain*, Igaku Shoin, Tokyo
19. Murakami, M., and Kouyama, T. (2008) Crystal structure of squid rhodopsin. *Nature* **453**, 363-367
20. Okada, T., Fujiyoshi, Y., Silow, M., Navarro, J., Landau, E. M., and Shichida, Y. (2002) Functional role of internal water molecules in rhodopsin revealed by X-ray crystallography. *Proc Natl Acad Sci U S A* **99**, 5982-5987
21. Jager, S., Palczewski, K., and Hofmann, K. P. (1996) Opsin/all-trans-retinal complex activates transducin by different mechanisms than photolyzed rhodopsin. *Biochemistry* **35**, 2901-2908
22. Vogel, R., and Siebert, F. (2001) Conformations of the active and inactive states of opsin. *J Biol Chem* **276**, 38487-38493
23. Bellingham, J., Chaurasia, S. S., Melyan, Z., Liu, C., Cameron, M. A., Tarttelin, E. E., Iuvone, P. M., Hankins, M. W., Tosini, G., and Lucas, R. J. (2006) Evolution of melanopsin photoreceptors: discovery and characterization of a new melanopsin in nonmammalian vertebrates. *PLoS Biol* **4**, e254
24. Blackshaw, S., and Snyder, S. H. (1999) Encephalopsin: a novel mammalian extraretinal opsin discretely localized in the brain. *J Neurosci* **19**, 3681-3690
25. Nieto, P. S., Valdez, D. J., Acosta-Rodriguez, V. A., and Guido, M. E. (2011) Expression of novel opsins and intrinsic light responses in the mammalian retinal ganglion cell line RGC-5. Presence of OPN5 in the rat retina. *PLoS One* **6**, e26417
26. Vigh, B., Manzano, M. J., Zadori, A., Frank, C. L., Lukats, A., Rohlich, P., Szel, A., and David, C. (2002) Nonvisual photoreceptors of the deep brain, pineal organs and retina. *Histol Histopathol* **17**, 555-590
27. Liu, L., and Gudas, L. J. (2005) Disruption of the lecithin:retinol acyltransferase gene makes mice more susceptible to vitamin A deficiency. *J Biol Chem* **280**, 40226-40234
28. Nakane, Y., Ikegami, K., Ono, H., Yamamoto, N., Yoshida, S., Hirunagi, K., Ebihara, S., Kubo, Y., and Yoshimura, T. (2010) A mammalian neural tissue opsin (Opsin 5) is a deep brain photoreceptor in birds. *Proc Natl Acad Sci U S A* **107**, 15264-15268
29. Oishi, T., Yamao, M., Kondo, C., Haida, Y., Masuda, A., and Tamotsu, S. (2001) Multiphotoreceptor and multioscillator system in avian circadian organization. *Microsc Res Tech* **53**, 43-47
30. Dacey, D. M., Liao, H. W., Peterson, B. B., Robinson, F. R., Smith, V. C., Pokorny, J., Yau, K. W., and Gamlin, P. D. (2005) Melanopsin-expressing ganglion cells in primate retina signal colour and irradiance and project to the LGN. *Nature* **433**, 749-754
31. Provencio, I., Rodriguez, I. R., Jiang, G., Hayes, W. P., Moreira, E. F., and Rollag, M. D. (2000) A novel human opsin in the inner retina. *J Neurosci* **20**, 600-605
32. Wade, P. D., Taylor, J., and Siekevitz, P. (1988) Mammalian cerebral cortical tissue responds to low-intensity visible light. *Proc Natl Acad Sci U S A* **85**, 9322-9326
33. Oishi, T., and Ohashi, K. (1993) Effects of Wavelengths of Light on the Photoperiodic Gonadal Response of Blinded-

Pinealectomized Japanese-Quail. *Zool Sci* **10**, 757-762
34. Kim, J. E., Tauber, M. J., and Mathies, R. A. (2001) Wavelength dependent cis-trans isomerization in vision. *Biochemistry* **40**, 13774-13778
35. Forger, N. G. (2009) Control of cell number in the sexually dimorphic brain and spinal cord. *J Neuroendocrinol* **21**, 393-399
36. Morrison, S. F., Nakamura, K., and Madden, C. J. (2008) Central control of thermogenesis in mammals. *Exp Physiol* **93**, 773-797
37. Cajochen, C., Munch, M., Kobialka, S., Krauchi, K., Steiner, R., Oelhafen, P., Orgul, S., and Wirz-Justice, A. (2005) High sensitivity of human melatonin, alertness, thermoregulation, and heart rate to short wavelength light. *J Clin Endocrinol Metab* **90**, 1311-1316
38. Hattar, S., Lucas, R. J., Mrosovsky, N., Thompson, S., Douglas, R. H., Hankins, M. W., Lem, J., Biel, M., Hofmann, F., Foster, R. G., and Yau, K. W. (2003) Melanopsin and rod-cone photoreceptive systems account for all major accessory visual functions in mice. *Nature* **424**, 76-81
39. Panda, S., Provencio, I., Tu, D. C., Pires, S. S., Rollag, M. D., Castrucci, A. M., Pletcher, M. T., Sato, T. K., Wiltshire, T., Andahazy, M., Kay, S. A., Van Gelder, R. N., and Hogenesch, J. B. (2003) Melanopsin is required for non-image-forming photic responses in blind mice. *Science* **301**, 525-527
40. Hoffman, R. A., and Reiter, R. J. (1965) Pineal Gland: Influence on Gonads of Male Hamsters. *Science* **148**, 1609-1611
41. Sung, C. H., Schneider, B. G., Agarwal, N., Papermaster, D. S., and Nathans, J. (1991) Functional heterogeneity of mutant rhodopsins responsible for autosomal dominant retinitis pigmentosa. *Proc Natl Acad Sci U S A* **88**, 8840-8844

FIGURE LEGENDS

Fig. 1. Characterization of the anti-mammalian Opn5m antibodies by western blotting. Signals were detected in Opn5m-transfected cells but not in mock-transfected cells. Recombinant mammalian Opn5m proteins exhibited two bands, probably because of the heterogeneity of the post-translational modification within the cultured cells, such as the glycosylation in the N-terminus of the protein, as shown for recombinant bovine rhodopsin (41).

Fig. 2. Comparison of the ability to directly bind 11-*cis*- or all-*trans*-retinal in vertebrate Opn5m proteins. (A-E) Absorption spectra of human (A), mouse (B), chicken (C), *Xenopus tropicalis* (D) and zebrafish (E) Opn5m proteins after incubation with 11-*cis*-retinal. Spectra were measured in the dark (curve 1), and after UV light irradiation (curve 2), subsequent yellow light (>500 nm) irradiation (curve 3), UV light re-irradiation (curve 4) or yellow light re-irradiation (curve 5). (*inset*) The calculated absorption spectra of each Opn5m protein in the dark (curve 1) and after UV light irradiation (curve 2). (F-J) Absorption spectra of human (F), mouse (G), chicken (H), *Xenopus* (I) and zebrafish (J) Opn5m proteins after incubation with all-*trans*-retinal. Spectra were measured in the dark (curve 1), and after yellow light (>500 nm) irradiation (curve 2), subsequent UV light irradiation (curve 3) or yellow light re-irradiation (curve 4). (K) Retinal configuration changes by UV light irradiation of human Opn5m. (left-hand panel) The retinal configurations were analyzed with HPLC after extraction of the chromophore as retinal oximes (syn and anti forms of 9-*cis*-, 11-*cis*-, and all-*trans*-retinal oximes). (right-hand panel) Isomeric compositions of retinal before and after light irradiation of human Opn5m.

Fig. 3. Time courses of G protein activation ability of mouse Opn5m. Gi activation ability of mouse Opn5m reconstituted with 11-*cis*-retinal was measured in the dark (circles), after UV light irradiation (squares), and after subsequent yellow light (>500 nm) irradiation (triangles). Data are presented as the means ± SEM of three independent experiments.

Fig. 4. Alteration of the ability to directly bind all-*trans*-retinal in mouse and *Xenopus* Opn5m mutants. (A) Spectral changes of mouse Opn5m proteins caused by orange light (>550 nm) irradiation. Extracts containing wild-type, T94S, T168A, D177S and I204V of mouse Opn5m with 1 % DM after reconstitution with all-*trans*-retinal were irradiated and then the difference spectra before and after irradiation were calculated. Each panel contains the spectra of wild-type (black curve) and mutant (red curve). (B) Modulation of the ability to directly bind all-*trans*-retinal by a single

mutation at position 168. Absorption spectra of wild-type and mutant of mouse and *Xenopus* Opn5m reconstituted with all-*trans*-retinal were measured in the dark (black curve) and after yellow light (>500 nm) irradiation (red curve).

Fig. 5. Expression of *Opn5m* and *Rpe65* mRNA in the mouse retina. (A-F) Detection of *Opn5m* mRNA in the retina of adult (ICR strain, 8 weeks, male), post-natal day 11 (P11) and P1 mouse. (D-F) Sense probes gave essentially no signals. (G-I) Detection of *Rpe65* mRNA in the RPE of adult, P11 and P1 mouse. (I) *Rpe65* mRNA was undetectable in P1 retina. Rpe, retinal pigment epithelium; Onl, outer nuclear layer; Inl, inner nuclear layer; Gcl, ganglion cell layer; Ob, outer neuroblastic layer; Ib, inner neuroblastic layer. Scale bar: 0.2 mm in (A-F); 0.2 mm in (G-I).

Fig. 6. Localization of Opn5m-expressing cells in the mammalian retina. Immunostaining of adult mouse (A, B) and common marmoset (C, C', D) retina. (B, D) When using the antibody preadsorbed with the antigenic peptide, there were no signals except weak signals in the GCL in (B) and photoreceptor cell layer in (D). Asterisk and arrow in (C) show Opn5m-expressing cells enlarged in (C'). Onl, outer nuclear layer; Inl, inner nuclear layer; Gcl, Ganglion cell layer; Prl, photoreceptor layer. Scale bars: 50 μm in (A, B); 25 μm in (C, C', D).

Fig. 7. Expression of Opn5m and Rpe65 in the mammalian brain. (A-D) Detection of *Opn5m* mRNA in the preoptic area. Coronal sections of mouse brain (ICR strain, female, 12 weeks) at the hypothalamus level. Approximate Bregma levels are 0.50 mm (A-C) and 0.14 mm (D). Large magnifications of (A) are shown in (B) as indicated. *Opn5m* mRNA was exclusively detected in the median preoptic nucleus and medial preoptic area at the anterior hypothalamus as shown in (A, B, D). C, Sense probe did not give rise to any staining. D, a small number of *Opn5m*-expressing cells were detected in the medial preoptic area (arrows) at the level of the posterior part of the anterior commissure. Scale bars: 2 mm in (A); 500 μm in (B, C); 2 mm in (D). cc, corpus callosum; Cpu, caudate putamen (striatum); aca, anterior commissure, anterior part; MnPO, median preoptic nucleus; MPA, medial preoptic area; 3v, third ventricle; och, optic chiasm; acp, anterior commissure. (E-H) Detection of *Rpe65* mRNA near the *Opn5m*-expression domain in the mouse brain (approximate lateral level, 0.36 mm). The arrows show the localization of *Opn5m* mRNA in the medial optic area (E, F), and *Rpe65* mRNA (G, H) in the olfactory tubercle. Scale bars: 2 mm in (E, G); 0.2 mm in (F, H). Lv, lateral ventricle; 3v, third ventricle; ac, anterior commissure; MPA, medial preoptic area; Tu, olfactory tubercle. (I-N) Detection of *Opn5m* and *Rpe65* mRNA in the common marmoset anterior hypothalamus. *Opn5m* mRNA was expressed in the anterior part of the medial preoptic area (MPO) (I, J) medially to the diagonal band (DB). Boxed area in I is magnified in J. Opn5m-positive cells were observed only in the anterior-most part of the MPO. *Rpe65* mRNA was detected in the paraventricular nucleus (Pa) of the anterior hypothalamus, slightly caudal to the Opn5m-positive cells (L, M). Boxed area in L is magnified in M. Signals were not detected with sense probes (K, N). Scale bars: 1 mm in (I, L); 200 μm in (J, M); 500 μm in (K, N). (O, P) Expression of Opn5m and RPE65 proteins in the mouse brain analyzed by western blotting. Opn5m protein was detected in the neural retina, hypothalamus and other brain area, not in the RPE, lung or liver (O). REP65 protein was detected in the RPE, hypothalamus and other brain area, not in the lung or liver (P).

Fig. 8. Expression of *Opn5m* mRNA in the mouse posterior hypothalamus and hippocampus. Coronal sections of mouse brain (ICR strain, female, 12 weeks) at the posterior hypothalamus (A, B) and hippocampus (C, D) levels. Approximate Bregma levels are -0.58 mm (A, B), and -1.34 mm (C, D). Large magnifications of (A, C) are shown in (B, D) as indicated. (A, B) At the posterior hypothalamus, *Opn5m* mRNA was not detected in the paraventricular nucleus along the third ventricle. (C, D) *Opn5m* mRNA was not detectable in the hippocampus. vhc, ventral hippocampal commissure; sm, stria medullaris; 3v, third ventricle; f, fornix; fi, fimbria of the hippocampus; Lv, lateral ventricle; ic, internal capsule; cc, corpus callosum; CA3, field CA3 of the hippocampus; MHb, medial habenular nucleus. Scale bars: 2 mm in (A, C); 500 μm in (B, D).

Fig. 9. Localization of RPE65-immunoreactive cells in the chick brain. (A) Opn5m-expressing neurons in the paraventricular organ (PVO).

There were no RPE65-immunoreactive cells in and near the PVO. (B) In the anterior hypothalamus, a subset of ependymal cells were immunoreactive for RPE65. The arrow shows RPE65 protein localized to the apical side of an ependymal cell. (C) More intense expression of RPE65 protein was observed in the ependymal cells lining the ventral region of the third ventricle (arrowheads). (D) The anti-RPE65 antibody recognized retinal pigment epithelium (Rpe) in the retina at P10. (E) To better visualize nuclei of RPE cells, blue channel is enhanced. Nuclei are stained with DAPI. 3v, third ventricle; Arc, arcuate nucleus; Me, median eminence; Os, outer segments of photoreceptors; Onl, outer nuclear layer; Inl, inner nuclear layer. Scale bar: 25 μm.

Fig. 10. Expression of *Opn5m* mRNA (arrows in A, C) in the mouse anterior hypothalamus (Bregma 0.50 mm level). (A, B) from male (C57BL6 strain, 8 weeks), (C, D) from female (C58BL6, 8 weeks). Higher magnification of (A, C; arrows) is shown in (B, D), respectively. The expression pattern appeared similar between the two sexes. aca, anterior commissure, anterior part; 3v, third ventricle. Scale bars: 2 mm in (A, C); 0.2 mm in (B, D).

Table 1. Comparison of the amino acid residues among vertebrate Opn5m proteins

Residue No.	bovine rhodopsin[b]	squid rhodopsin	zebrafish Opn5m	*Xenopus* Opn5m	chicken Opn5m	platypus/opossum Opn5m	mouse/human Opn5m
94[a]	T	M	F	A	S	T	T
168	A	A	A	A	A	A	T
177	R	A	N	N	S	N	D
204	V	I	V	V	V	I	I

[a] Amino acid residue numbers are designated using the bovine rhodopsin numbering system.
[b] NCBI accession numbers of opsin sequences are as follows: bovine rhodopsin, K00506; squid rhodopsin, X70498; platypus Opn5m, XM_001511941; opossum Opn5m, XM_001369165.

Figure 1

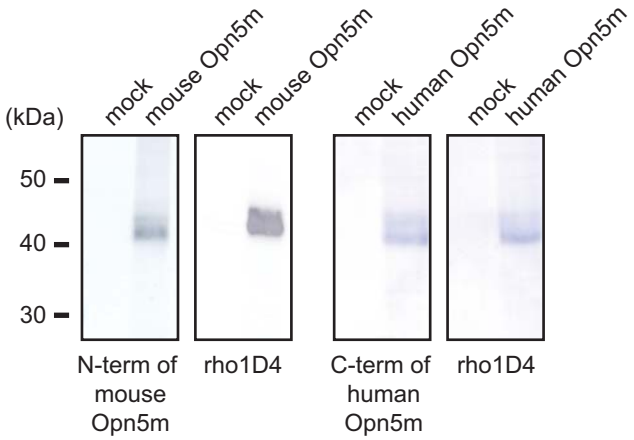
mock
mouse Opn5m
mock
mouse Opn5m
mock
human Opn5m
mock
human Opn5m
(kDa)
50
40
30
N-term of mouse Opn5m
rho1D4
C-term of human Opn5m
rho1D4

Figure 2

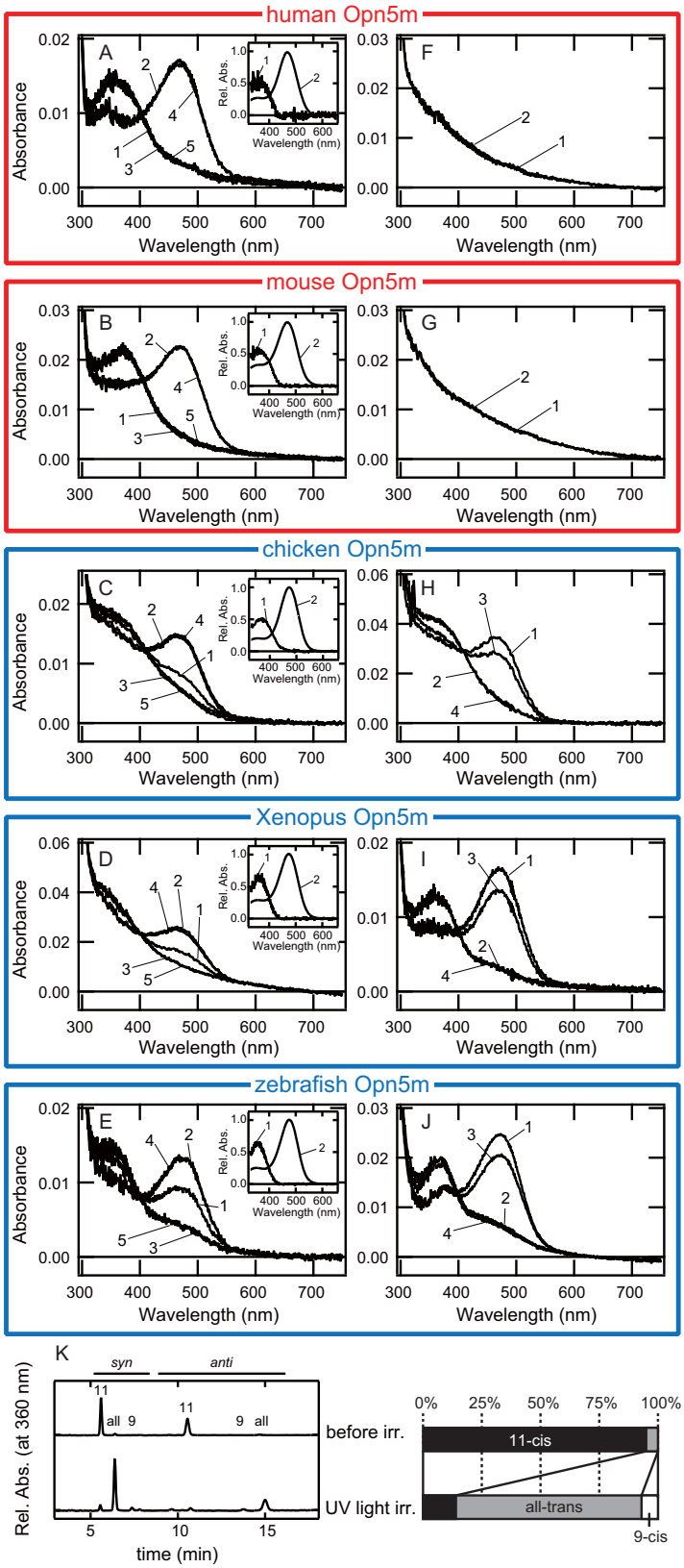
human Opn5m
mouse Opn5m
chicken Opn5m
Xenopus Opn5m
zebrafish Opn5m
Absorbance
Rel. Abs.
Wavelength (nm)
A
B
C
D
E
F
G
H
I
J
K
Rel. Abs. (at 360 nm)
time (min)
syn
anti
all 9
11
9 all
before irr.
UV light irr.
0%
25%
50%
75%
100%
11-cis
all-trans
9-cis

Figure 3

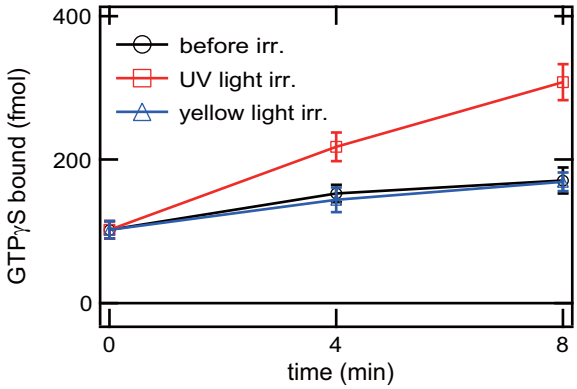
400
200
0
GTPγS bound (fmol)
before irr.
UV light irr.
yellow light irr.
0
4
8
time (min)

Figure 4

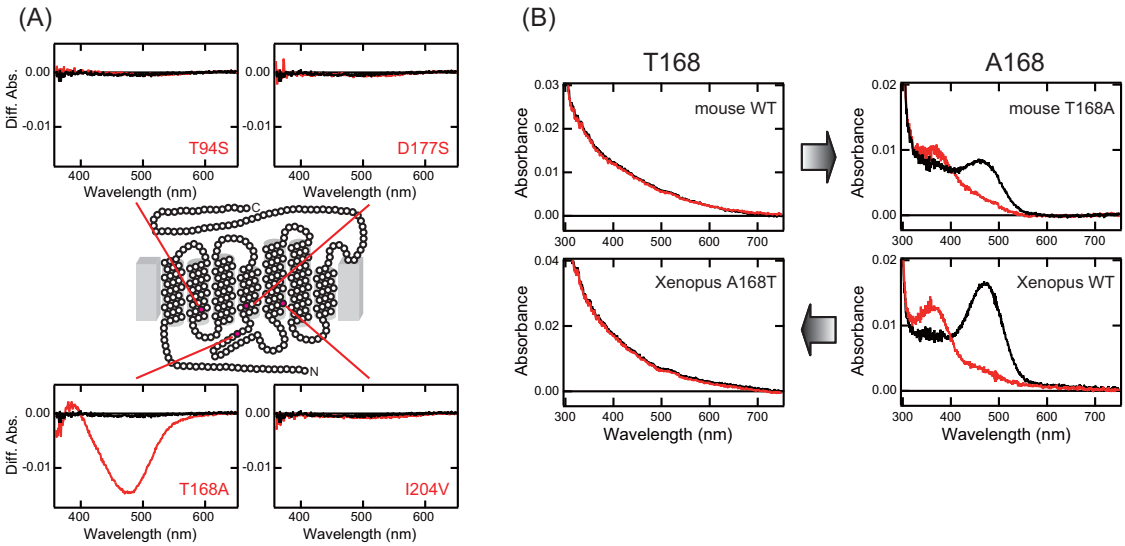
(A)
Diff. Abs.
0.00
-0.01
T94S
D177S
400
500
600
Wavelength (nm)
C
N
T168A
I204V
(B)
T168
A168
mouse WT
mouse T168A
Xenopus A168T
Xenopus WT
Absorbance
0.03
0.02
0.01
0.00
0.04
300
700

Figure 5

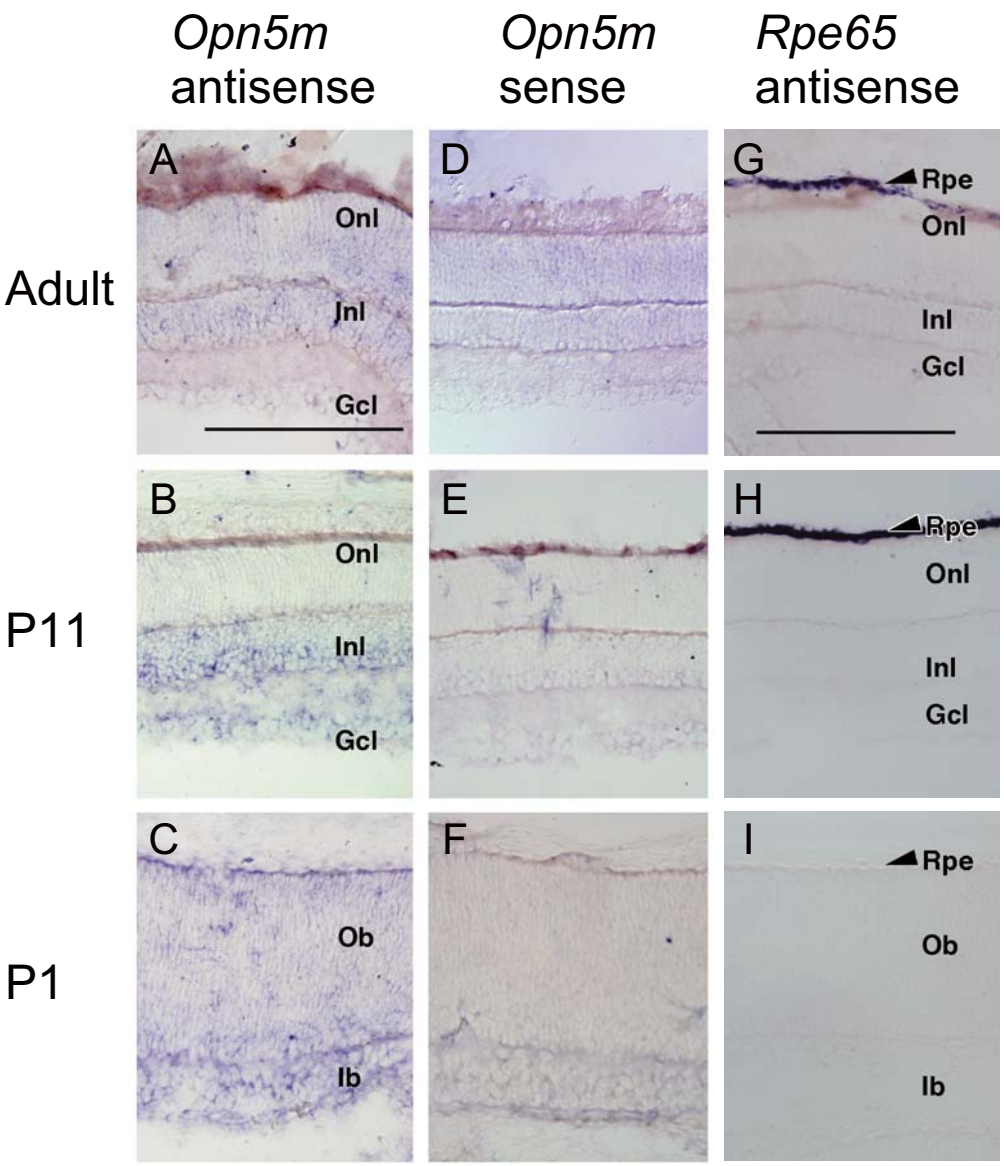
Opn5m antisense
Opn5m sense
Rpe65 antisense
Adult
P11
P1
A
B
C
D
E
F
G
H
I
Onl
Inl
Gcl
Ob
Ib
Rpe

Figure 6

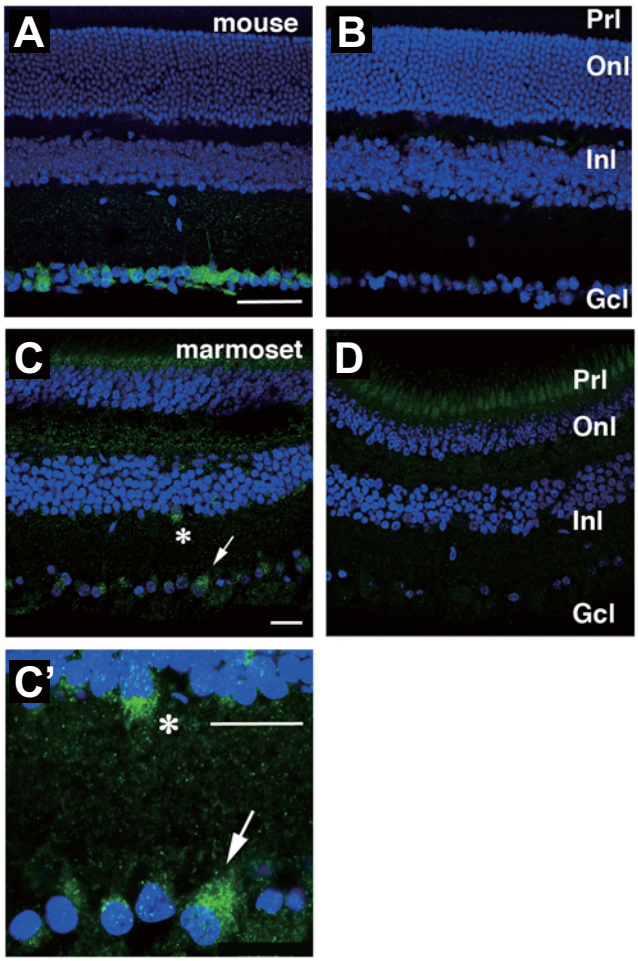

Figure 7

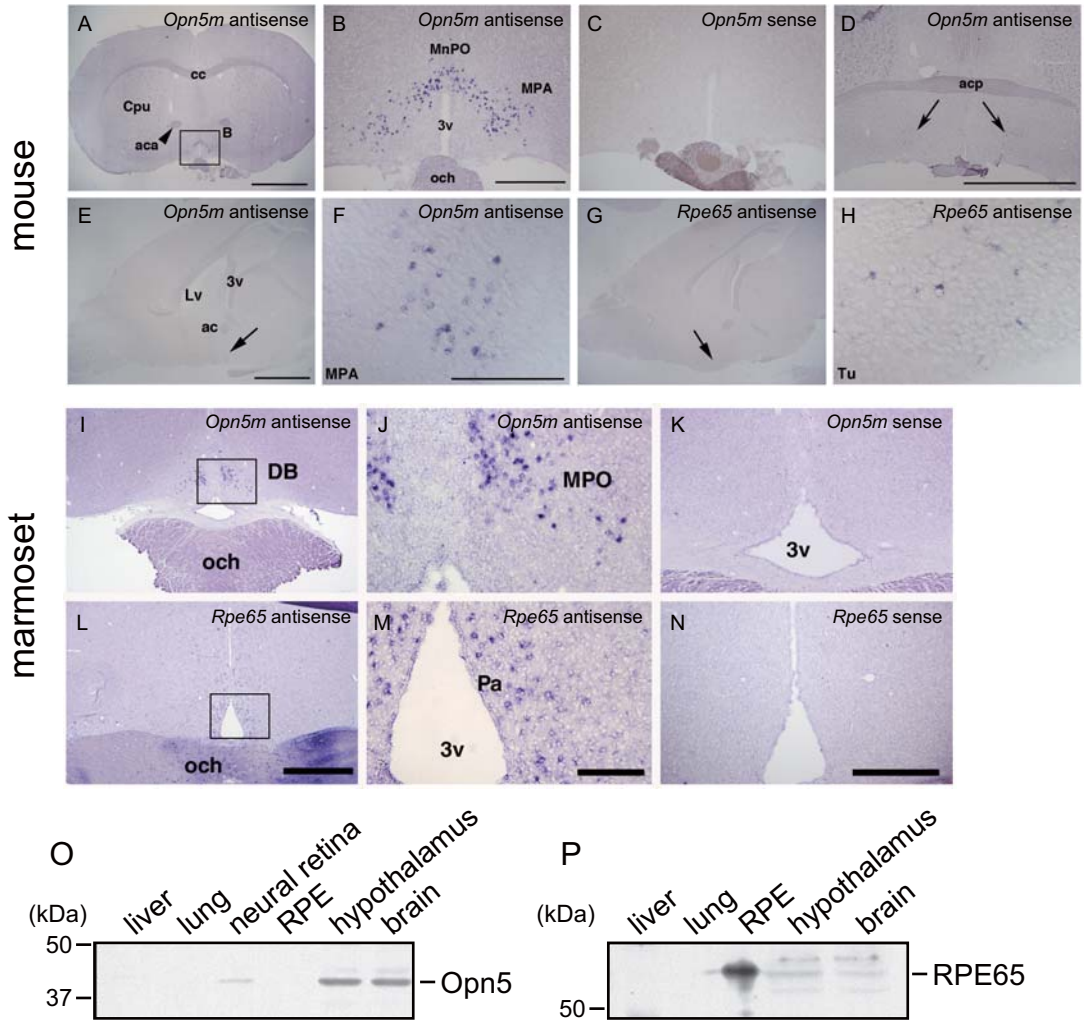
mouse
A
Opn5m antisense
cc
Cpu
aca
B
B
Opn5m antisense
MnPO
MPA
3v
och
C
Opn5m sense
D
Opn5m antisense
acp
E
Opn5m antisense
Lv
3v
ac
F
Opn5m antisense
MPA
G
Rpe65 antisense
H
Rpe65 antisense
Tu
marmoset
I
Opn5m antisense
DB
och
J
Opn5m antisense
MPO
K
Opn5m sense
3v
L
Rpe65 antisense
och
M
Rpe65 antisense
Pa
3v
N
Rpe65 sense
O
(kDa)
liver
lung
neural retina
RPE
hypothalamus
brain
50
37
Opn5
P
(kDa)
liver
lung
RPE
hypothalamus
brain
50
RPE65

Figure 8

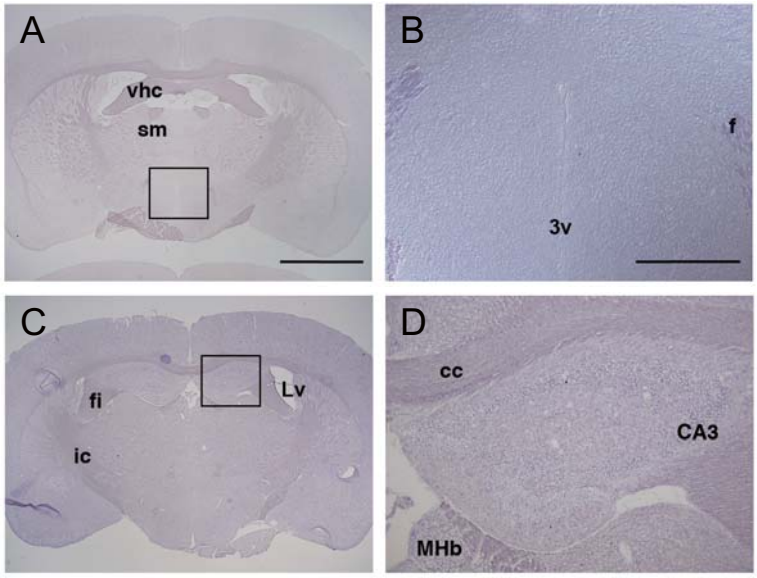

Figure 9

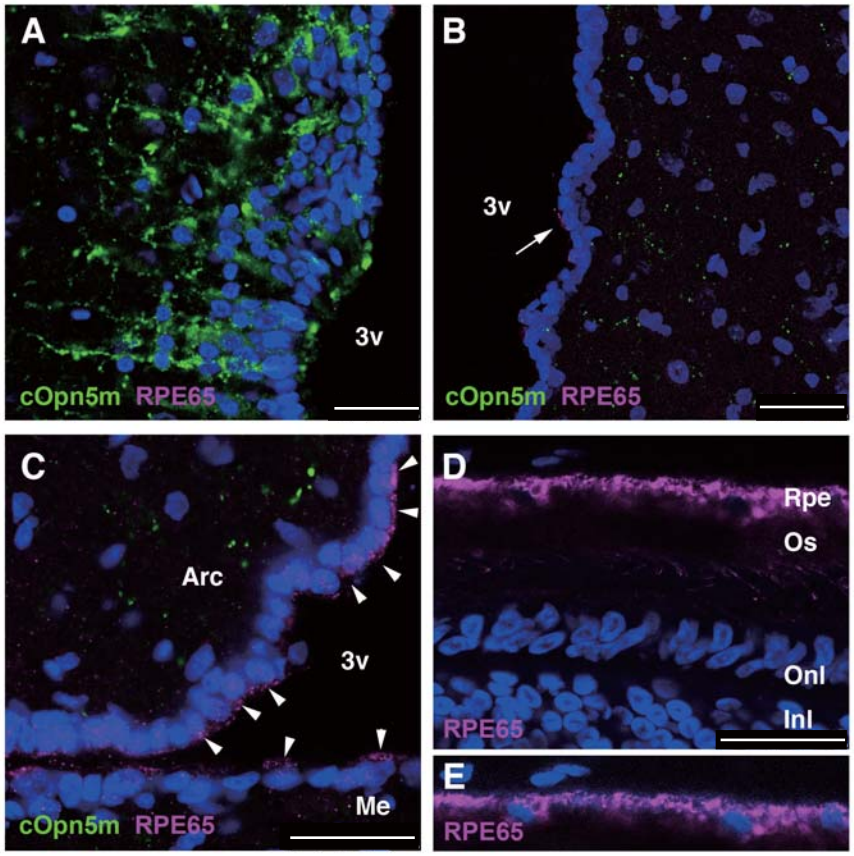
A
3v
cOpn5m RPE65
B
3v
cOpn5m RPE65
C
Arc
3v
Me
cOpn5m RPE65
D
Rpe
Os
Onl
Inl
RPE65
E
RPE65

Figure 10